

Guided plasmons in graphene p - n junctions

E. G. Mishchenko,¹ A. V. Shytov*,¹ and P. G. Silvestrov²

¹*Department of Physics and Astronomy, University of Utah, Salt Lake City, Utah 84112, USA*

²*Theoretische Physik III, Ruhr-Universität Bochum, 44780 Bochum, Germany*

Spatial separation of electrons and holes in graphene gives rise to existence of plasmon waves confined to the boundary region. Theory of such guided plasmon modes within hydrodynamics of electron-hole liquid is developed. For plasmon wavelengths smaller than the size of charged domains plasmon dispersion is found to be $\omega \propto q^{1/4}$. Frequency, velocity and direction of propagation of guided plasmon modes can be easily controlled by external electric field. In the presence of magnetic field spectrum of additional gapless magnetoplasmon excitations is obtained. Our findings indicate that graphene is a promising material for nanoplasmonics.

PACS numbers: 73.23.-b, 72.30.+q

Introduction. Breakthrough progress in synthesis and characterization has made graphene [2] a promising object for nanoelectronics. Operation of graphene-based transistors [3] and other components would rely on the properties of its *single-particle* excitations – electrons and holes. However, one can also envisage a completely different set of applications which employ *collective* excitations, such as plasmons. Currently, plasmon excitations in metallic structures are a subject of nanoplasmonics, a new field which has emerged at the confluence of optics and condensed matter physics with one of the aims being the developing of plasmon-enhanced high resolution near-field imaging methods [4, 5]. Another objective is possible utilization of plasmons in integrated optical circuits. However, perspectives of graphene for nanoplasmonics are largely unexplored since plasmon modes of graphene flakes have not been addressed so far. As our results indicate a great amount of control over graphene plasmon properties makes it a very promising material for applications.

Fundamentally, the spectrum of collective charge oscillations reflects the long-range nature of Coulomb interaction. In conventional two dimensional systems, such as those created in semiconducting heterostructures, plasmons are gapless, $\omega^2(q) = 2\pi e^2 n q / m^*$, with n and m^* being electron density and effective mass, respectively [6]. Such oscillations can be treated hydrodynamically. In clean graphene at zero temperature the plasmon frequency, $\omega^2 \propto |E_F|$, vanishes with decreasing the doping level E_F . It has been argued [7] that the interaction between electrons and holes in the final state can modify the response functions of Dirac fermions and open up a possibility for the propagation of charge oscillations at low frequencies $\omega < qv$, where v is electron velocity. Still, hydrodynamic ($\omega > qv$) analog of conventional plasmons remains absent unless either temperature is non-zero [8] or graphene is driven away from the charge neutrality point by doping or gating [9]. Expectedly, in both cases plasmon spectrum has the conventional form, $\omega(q) \propto q^{1/2}$.

In the present paper we investigate spectra of hydrodynamic plasmons in spatially inhomogeneous graphene

flakes. Realistic graphene samples are typically subject to disorder potential and mechanical strain [10] that lead to the formation of charged electron and hole puddles [11] with boundaries between n and p regions being the lines of zero chemical potential. Moreover, controlled p - n junctions can be made with the help of metallic gates [12]. Also p - n junctions can be created by applying electric field within the plane of a graphene flake, see Fig. 1a. The field separates electrons and holes spatially in a way that allows control of both the amount of induced charge (and thus plasmon frequency) and spatial orientation of the junction (the direction of plasmon propagation).

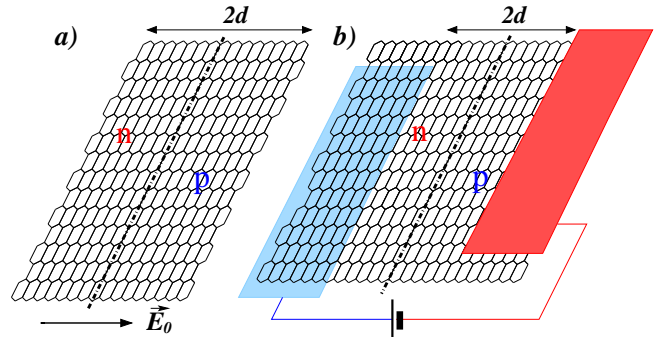


FIG. 1: Two types of graphene p - n junctions: a) field-induced, b) gate-induced. Dot-dashed line indicates boundary between electron and hole regions and, correspondingly, the direction of plasmon propagation. In case of field-induced junction it is controlled by the direction of external electric field E_0 .

Below, we demonstrate that such p - n junctions can guide plasmons. We show the existence of charge oscillations which are localized at the junction and have the amplitude decaying with the distance to the junction. For wavelengths shorter than the width of the charged domains, we find the plasmon spectrum of the form,

$$\omega_n^2(q) = \alpha_n \frac{e^2 v}{\hbar} \sqrt{\frac{q |\rho'_0|}{e}}, \quad (1)$$

where ρ'_0 is the gradient of equilibrium charge density at the junction, v is electron velocity, and $n = 0, 1, 2, \dots$

enumerates the solutions. The lowest mode has $\alpha_0 = 4\sqrt{2}\pi\Gamma(3/4)/\Gamma(1/4) \approx 3.39$.

Below we derive this result and discuss plasmon properties for the two types of p - n junctions: electric field controlled and gate controlled, as shown in Fig. 1.

Hydrodynamics of charge density oscillations. We utilize the hydrodynamic approach to describe the motion of charged Dirac fermions. The rate of change of electric current density \mathbf{J} due to dynamic electric field \mathbf{E} follows from the usual intra-band Drude conductivity with the corresponding density of states [13],

$$\dot{\mathbf{J}}(\mathbf{r}, t) = \frac{e^2}{\pi\hbar^2} |\mu(\mathbf{r})| \mathbf{E}(\mathbf{r}, t), \quad (2)$$

determined by the local value of chemical potential $\mu(\mathbf{r})$ as measured from the Dirac point (positive for electrons and negative for holes). Electric current is related to the variation of charge density $\delta\rho$ by means of the continuity equation,

$$\delta\dot{\rho}(\mathbf{r}, t) + \nabla \cdot \mathbf{J}(\mathbf{r}, t) = 0. \quad (3)$$

Finally, the variation of charge density produces electric field according to the Coulomb law [14],

$$\mathbf{E}(\mathbf{r}, t) = -\nabla \int d^2r' \frac{\delta\rho(\mathbf{r}', t)}{|\mathbf{r} - \mathbf{r}'|}. \quad (4)$$

Equations (2)-(4) give a closed system for plasmon excitations in graphene flakes. We apply it to a p - n junction created in a strip infinite along the y -axis (direction of plasmon propagation). Using the Fourier representation, $\delta\rho(\mathbf{r}, t) = \delta\rho(x) \exp(iqy - i\omega t)$, and eliminating \mathbf{E} and \mathbf{J} we arrive at the equation for the oscillating part of electron density,

$$\omega^2 \delta\rho(x) + \frac{2e^2 v}{\sqrt{\pi}\hbar} \left\{ \frac{d}{dx} \sqrt{\frac{|\rho_0(x)|}{e}} \frac{d}{dx} - q^2 \sqrt{\frac{|\rho_0(x)|}{e}} \right\} \times \int_{-d}^d dx' \delta\rho(x') K_0(|q||x - x'|) = 0, \quad (5)$$

Here K_0 is the modified Bessel function and $2d$ is the width of graphene flake. Within the Thomas-Fermi approximation equilibrium charge density $\rho_0(x)$ is related to the chemical potential via $\rho_0(x) = -\text{sgn}(\mu) e \mu^2(x) / \pi \hbar^2 v^2$ (electron charge is taken to be $-e$). This follows from the condition that the electrochemical potential $\mu(x) - e\phi(x)$ is constant throughout the system. The solutions of Eq. (5) will now be considered for large and small plasmon momenta separately.

Short wavelength, $q \gg 1/d$. In this case the decay of plasmon density $\delta\rho(x)$ occurs over a distance much smaller than the width of the system and the limits of integration in Eq. (5) can be extended to infinity. Assuming (cf. Eq. (11) below) the linear dependence, $\rho_0(x) = \rho'_0 x$, we observe that the integro-differential

equation (5) acquires obvious scaling property. Introducing the variable $\xi = qx$ we arrive at the plasmon spectrum in the form (1), with dimensionless constants α_n determined from the eigenvalue problem:

$$-\frac{2}{\sqrt{\pi}} \left(\frac{d}{d\xi} \sqrt{|\xi|} \frac{d}{d\xi} - \sqrt{|\xi|} \right) \times \int_{-\infty}^{\infty} d\xi' \delta\rho^{(n)}(\xi') K_0(|\xi - \xi'|) = \alpha_n \delta\rho^{(n)}(\xi). \quad (6)$$

Interestingly, this integro-differential equation allows a complete analytic solution, though the detailed analysis is beyond the scope of this paper. Our main findings are as follows. Solutions are enumerated by $n = 0, 1, 2, \dots$ with even/odd numbers corresponding to even/odd density profile, $\delta\rho^{(n)}(-\xi) = (-1)^n \delta\rho^{(n)}(\xi)$. Surprisingly, eigenvalues are *doubly-degenerate* and given by

$$\alpha_{2n} = \alpha_0 \frac{2n+1}{4n+1} \cdot \frac{3 \cdot 7 \cdot \dots (4n-1)}{1 \cdot 5 \cdot \dots (4n-3)}, \quad \alpha_{2n+1} = \alpha_{2n}. \quad (7)$$

At large distances all modes have exponential dependence, $\delta\rho^{(n)}(\xi) \sim e^{-|\xi|}$, while at $|\xi| \ll 1$ even and odd solutions exhibit different behavior, $\delta\rho^{(\text{even})} \sim 1 - \text{const}\sqrt{|\xi|}$ and $\delta\rho^{(\text{odd})} \sim \text{sign}(\xi)/\sqrt{|\xi|}$. The first pair of solutions (belonging to the lowest eigenvalue α_0) in the Fourier representation $\delta\rho^{(n)}(k) = \int d\xi \delta\rho^{(n)}(\xi) e^{ik\xi}$ acquires a simple form:

$$\delta\rho^{(0)}(k) \propto \frac{1}{(1+k^2)^{3/4}}, \quad \delta\rho^{(1)}(k) \propto \frac{k}{(1+k^2)^{3/4}}. \quad (8)$$

Long wavelength, $q \ll 1/d$. In contrast to the above result (1) plasmon spectrum at small q is sensitive to a specific realization of the p - n junction. We address the long-wavelength behavior of plasmons in field controlled junctions. We expect this case to be of more interest, in addition it allows a more complete description. Before analyzing plasmons in this structure, we discuss the equilibrium density profile. As shown in Fig. 1a the flake of width $2d$ is placed in external electric field E_0 applied along the x -direction. The equilibrium density distribution $\rho(x)$ is found from,

$$E_0 x + \text{sgn}(x) \frac{\hbar v}{e} \sqrt{\frac{\pi}{e} |\rho_0(x)|} + 2 \int_0^d dx' \rho_0(x') \ln \frac{x+x'}{|x-x'|} = 0, \quad (9)$$

where it is used that $\rho_0(x) = -\rho_0(-x)$. Prior to solving Eq. (9) it is instructive to analyze validity of the semiclassical approach. The first condition implies that the change of the electron wavelength is smooth on the scale of itself, $d/dx(\hbar v/\mu) \ll 1$. Estimating $\mu(x) \sim eE_0 x$ we obtain that the distance to the p - n junction line ($x = 0$) should exceed the characteristic electric field length $l_E = \sqrt{e/E_0} \ll x$. The second condition requires that the electron wavelength is small compared with the width of the system, $d \gg \hbar v/\mu$. Noting that in graphene

$\hbar v \sim e^2$ we can rewrite this second condition simply as $l_E \ll d$. Thus, the Thomas-Fermi equation (9) for the equilibrium charge density and the hydrodynamic equation (5) for its variation are applicable as long as

$$l_E \ll d, \quad q \ll 1/l_E. \quad (10)$$

However, the ratio of q and $1/d$ can be arbitrary. For a moderate external electric field $\sim 10^4 \text{V/m}$ the value of electric length $l_E \sim 0.4 \mu\text{m}$ and the first of the conditions (10) is satisfied easily for micron-sized samples.

Analytic solution of Eq. (9) is possible when the second term is small, in which case the charge density is [15]

$$\rho_0(x) = \frac{E_0 x}{\sqrt{d^2 - x^2}}. \quad (11)$$

Substituting this expression back into Eq. (9) we observe that the second term is indeed negligible as long as $x \gg l_E^2/d$. This is assured whenever the conditions (10) are satisfied. It is also worth pointing out that Eq. (11) justifies the linear approximation for the charge density used in deriving Eq. (1) for $q \gg 1/d$, with $\rho'_0/e = 1/(l_E^2 d)$.

We now turn to the analysis of plasma oscillations propagating on top of the density distribution, Eq. (11). For small plasmon momenta, $q \ll 1/d$, electric field extends beyond the width of the flake and the equation (5) needs to be supplemented with the boundary condition, which ensures that electric field (and thus the current) vanishes at the edges, $x = \pm d$:

$$\text{P} \int_{-d}^d dx \frac{\delta \rho(x)}{x \pm d} = 0. \quad (12)$$

The spectrum of the lowest symmetric mode can be most easily found by integrating Eq. (5) across the width of the flake. The first term in the brackets will then vanish exactly due to the boundary condition (12). The remaining integral can now be calculated to the logarithmic accuracy with the help of the approximation $K_0(q|x-x'|) = -\ln q|x-x'|$:

$$\int_{-d}^d dx \sqrt{\frac{|\rho_0(x)|}{e}} \ln(q|x-x'|) \approx \frac{2d\Gamma^2(3/4)}{l_E\sqrt{\pi}} \ln(qd). \quad (13)$$

Eqs. (5) and (13) combine to give the equation, $[\omega^2 - \omega_0^2(q)] \int_{-d}^d dx \delta \rho(x) = 0$, that yields the dispersion of the gapless symmetric plasmon,

$$\omega_0^2(q) = \Gamma^2(3/4) \frac{4e^2 v d}{\pi \hbar l_E} q^2 \ln(1/qd), \quad (14)$$

reminiscent of the plasmon spectrum in quasi-one-dimensional wires. The remaining modes, $n \geq 1$, are gapped. For these modes $\int_{-d}^d dx \delta \rho(x) = 0$ and simple procedure of integrating Eq. (5) over the width of the

flake is not useful. Instead, the equation for the n -th frequency gap can be obtained by setting $q = 0$ in Eq. (5). We observe that

$$\omega_n^2(0) = \beta_n \frac{e^2 v}{\hbar l_E d}, \quad (15)$$

where β_n are the eigenvalues of the equation,

$$\frac{2}{\sqrt{\pi}} \frac{d}{d\xi} \frac{\sqrt{|\xi|}}{(1-\xi^2)^{1/4}} \int_{-1}^1 d\xi' \frac{\delta \rho^{(n)}(\xi')}{\xi - \xi'} = \beta_n \delta \rho^{(n)}(\xi). \quad (16)$$

The zeroth mode $\beta_0 = 0$, see Eq. (14), is found analytically: $\delta \rho^{(0)} \propto 1/\sqrt{1-\xi^2}$. It describes charge distribution in the strip in response to a (uniform along x direction and smooth along y -direction) change of its chemical potential [16]. Other solutions of Eq. (16) are found numerically:

$$\beta_1 = 1.41, \quad \beta_2 = 6.49, \quad \beta_3 = 6.75, \dots \quad (17)$$

With increasing n the eigenmodes of integro-differential equation (16) oscillate faster, but in general do not follow the oscillation theorem familiar from quantum mechanics. In particular, the solutions with $n = 0$ and $n = 3$ are even while $n = 1, n = 2$ are odd [17].

Finally, we mention the case of a gate-controlled p - n junction, Fig. 1b. The equilibrium density profile is linear near $x = 0$ and saturates for large $|x|$ [18]. Eq. (1) is still applicable for $q > 1/d$. In the limit $q < 1/d$ one should take into account the screening of long-range Coulomb interaction by metallic gates. In this case the logarithm in the spectrum of the gapless plasmon disappears, and the lowest mode Eq. (14) becomes sound-like.

Magnetoplasmons. If external magnetic field \mathbf{B} is applied perpendicularly to the plane of graphene the plasmon spectra acquire new modes. The equation of motion (2) should now be modified to include the Lorentz force,

$$\dot{\mathbf{J}}(\mathbf{r}, t) = \frac{e^2}{\pi \hbar^2} |\mu(x)| \mathbf{E}(\mathbf{r}, t) - \frac{ev^2}{c\mu(x)} \mathbf{J} \times \mathbf{B}. \quad (18)$$

The relative coefficient between electric and magnetic terms in this equation follows from the expression for the Lorentz force acting on a single particle. The last term has opposite sign for electrons and holes. Note that the frequency of cyclotron motion $\omega_B(x) = ev^2 B/c\mu(x)$ in graphene p - n junctions is position-dependent. The remaining equations (3)-(4) are intact in the presence of magnetic field. The boundary condition requires now the vanishing of the normal component of electric current at the boundary, rather than simply vanishing of the electric field, as in Eq. (12). Eliminating \mathbf{J} and \mathbf{E} we arrive at the generalization of equation (5),

$$\delta \rho(x) + \frac{2e^2}{\pi} \left\{ q^2 \mathcal{Z} - \frac{q}{\omega} (\omega_B \mathcal{Z})' - \frac{d}{dx} \mathcal{Z} \frac{d}{dx} \right\} \times \int_{-d}^d dx' \delta \rho(x') K_0(|q||x-x'|) = 0, \quad (19)$$

where $\mathcal{Z}(x) = |\mu(x)|/(\omega_B^2(x) - \omega^2)$.

The most interesting effect described by Eq. (19) is the appearance of a set of new modes, chiral magnetoplasmons, similar to those considered in Ref. [19] for conventional 2D electron systems with smooth boundaries. To find their dispersion in strong magnetic fields, when $\omega \ll \omega_B(x)$ (the exact condition is given below), one should retain only the second term in Eq. (19). Noticing that $(\omega_B \mathcal{Z})' = \pi l_B^2 \rho_0'(x)/e = \pi l_B^2/(l_E^2 d)$, where $l_B = \sqrt{\hbar c/eB}$ is the magnetic length, we arrive at the integral equation

$$-\frac{2c}{B} \frac{q}{\omega} \frac{d\rho_0(x)}{dx} \int_{-d}^d dx' \delta\rho(x') K_0(|q||x-x'|) = \delta\rho(x) \quad (20)$$

Since K_0 is positive, propagation of magnetoplasmons with $q > 0$ is quenched, indicative of their chiral property [20]. As seen from Eq. (20), the plasmon density $\delta\rho(x)$ is concentrated where $\rho_0'(x)$ is the strongest. The derivative of the charge density in *field-induced* junctions (11) features strong singularity near the edges of the flake. Thus, low-frequency magnetoplasmon spectrum is strongly dependent on the microscopic regularization of this singular behavior and is, therefore, beyond the scope of the Thomas-Fermi approximation used throughout this paper.

The *gate-induced* junctions, however, allow a rather simple analytical description of these modes if we approximate that $\rho_0'(x) = e/l_E^2 d$ for $|x| \leq d$ and $\rho_0'(x) = 0$ for $|x| > d$. The oscillating density $\delta\rho(x)$ then vanishes for $|x| > d$. The solution inside the strip, $|x| \leq d$, can be easily found for $q \gg 1/d$, where one can assume the range of integration in Eq. (20) to be infinite. The eigenfunctions of Eq. (20) are simply given by $\sin[q_\perp(x+d)]$, with the values of $q_\perp = \pi n/2d$ determined from the condition, $\delta\rho_q(\pm d) = 0$. The spectrum of magnetoplasmons is then found to be,

$$\omega_n(q) = -\frac{2\pi e^2 l_B^2}{\hbar l_E^2 d} \frac{q}{\sqrt{q^2 + \pi^2 n^2/4d^2}}, \quad n = 1, 2, \dots \quad (21)$$

The magnetoplasmon spectrum (21) is derived under the assumption that magnetic field is strong, $\omega_B(d) \gg \omega$, which implies that $l_B \ll l_E$. In order to neglect the first and third terms in the brackets in Eq. (19) one has to ensure that $q \ll (l_E/l_B)^4/d$. This condition might turn out to be more or less restrictive than the hydrodynamics condition $q \ll 1/l_E$, depending on the particular value of the ratio l_B/l_E . Note that the smallness of this ratio is not in contradiction to the non-quantized description of electron motion in magnetic field. The latter is valid as long as the filling factor is large, $eEd \gg \omega_B(d)$, which means that $l_B \gg l_E^2/d$. For magnetic field ~ 1 T, and $l_B \sim 25$ nm, using the estimate below Eq. (10) that $l_E \sim 400$ nm we conclude that the width of the flake should exceed $d > 10\mu\text{m}$. The magnetoplasmon modes (21) are $\sim (l_B/l_E)^2$ slower than electrons. Note that these modes

are undamped since single-particle excitations cannot be induced at frequencies below cyclotron frequency ω_B .

Conclusions. Graphene *p-n* junctions are among the most simple and promising applications of this material. Single-electron properties of *p-n* junctions have been extensively studied. In the present paper we investigated their collective excitations both with and without magnetic field. We anticipate that plasmon modes will be crucial for the optical response of graphene nanostructures and realistic samples containing electron-hole puddles. High degree of experimental control should make them of special interest to nanoplasmonics and electronics. Among the most promising applications of plasmons in *p-n* junctions we envisage a possibility of a ‘‘plasmon transistor’’ [4]. In particular, by simply switching the direction of electric field from across the flake to along it (and back) the propagation of plasmons can be facilitated (or prevented). In addition, as follows from the above Eqs. (1), (11), the plasmon velocity can be controlled with simple change in the magnitude of electric field. This is in a sharp contrast to plasmons in metallic nanostructures, whose spectra are typically fixed once devices are fabricated.

Acknowledgments. Useful discussions with M. Raikh and O. Starykh are gratefully acknowledged. This work was supported by DOE, Grant No. DE-FG02-06ER46313. P.G.S. was supported by the SFB TR 12.

-
- [*] Present address: School of Physics, University of Exeter, EX4 4QL, U.K.
 - [2] M. Wilson, Phys. Today **59**, No. 1, 21 (2006).
 - [3] A.K. Geim and K.S. Novoselov, Nature Mater. **6**, 183 (2007).
 - [4] H.A. Atwater, Sci. Am. **296**, 56 (2007).
 - [5] S.A. Maier, *Plasmonics: Fundamentals and Applications* (Springer, New York, 2007).
 - [6] F. Stern, Phys. Rev. Lett. **18**, 546 (1967).
 - [7] S. Gangadharaiyah, A.M. Farid, and E.G. Mishchenko, Phys. Rev. Lett. **100**, 166802 (2008).
 - [8] O. Vafek, Phys. Rev. Lett. **97**, 266406 (2006).
 - [9] E.H. Hwang and S. Das Sarma, Phys. Rev. B **75**, 205418 (2007).
 - [10] A.H. Castro Neto *et al.*, Rev. Mod. Phys. **81**, 109 (2009).
 - [11] J. Martin *et al.*, Nature Physics **4**, 144 (2008).
 - [12] J.R. Williams, L. DiCarlo, and C.M. Marcus, Science **317**, 638 (2007).
 - [13] Rigorous derivation of Eq. (2) is based on the ‘‘relativistic’’ stress energy-momentum tensor, see L.D. Landau and E. M. Lifshitz, *Fluid Mechanics*, Butterworth-Heinemann, Oxford (1987), Ch. 15; M. Mueller, L. Fritz, S. Sachdev, and J. Schmalian, arXiv:0810.3657.
 - [14] In the case of gate controlled junctions the image charges induced at the gates should be included into Eq. (4).
 - [15] T.A. Sedrakyan, E.G. Mishchenko, and M.E. Raikh, Phys. Rev. B **74**, 235423 (2006).
 - [16] P.G. Silvestrov and K.B. Efetov, Phys. Rev. B **77**, 155436 (2008).

- [17] In addition even and odd solutions with $n > 0$ have different singular behavior at $|\xi| \ll 1$: $\delta\rho^{(\text{even})} \sim \sqrt{|\xi|}$, $\delta\rho^{(\text{odd})} \sim \text{sign}(\xi)/\sqrt{|\xi|}$. At $\xi \rightarrow \pm 1$ all solutions diverge as $\delta\rho \sim 1/\sqrt{1-\xi^2}$.
- [18] L.M. Zhang and M.M. Fogler, Phys. Rev. Lett. **100**, 116804 (2008).
- [19] I.L. Aleiner and L.I. Glazman, Phys. Rev. Lett. **72**, 2935 (1994).
- [20] V.A. Volkov and S. A. Mikhailov, JETP Lett. **42**, 556 (1985).